RESEARCH PAPER

The effect of melting point depressant elements B, Si, and P in Ni-based brazing filler metals on the formation of brazed joints

Yubo Sun[1,2] · Zhiping Wang[1,2]

Abstract

Hastelloy X is extensively used in aero-engine hot-section components, which is mainly manufactured by brazing. The type of brazing filler metal has a direct influence on the performance of the brazed joint. In the present study, Hastelloy X is utilized as the base metal, and the B, Si, and P are utilized as the primary melting-point depressant (MPD) elements, respectively. The distribution and diffusion behavior of MPD elements is investigated. The microstructure forming characteristics of the brazed joint and the element distribution at the interface are analyzed. The influence of MPD elements in the brazing filler metal and their interaction with the base metal on the tensile strength of the joint is revealed. The results of the analysis indicated that the interaction layer in the BNi-2 containing B and Si exhibited the morphological feature of "thick in the middle and thin at both ends." The interaction layer thicknesses of the brazed joints containing B and Si (BNi-2), Si (BNi-5), and P (BNi-7) were 150 μm, 110 μm, and 80 μm, respectively; the corresponding tensile strengths were 581.69 MPa, 498.45 MPa, and 496.09 MPa, respectively. Thus, the joint strength increased with an increase in the thickness of the interaction layer, and brittle cleavage fractures were noted.

Keywords Brazing · Hastelloy X · Melting point depressants · Mechanical properties

1 Introduction

Ni-based superalloys exhibit excellent thermal strength and stability and are extensively used to manufacture hot section components, such as combustors and turbine disks of aeroengines. These components may undergo structural cracking due to thermal oxidation, corrosion, and fatigue [1–4]. Moreover, Ni-based alloys are typically composed of strengthening elements, such as Al and Ti, thereby increasing the difficulty of repairing components made of Ni-based alloys through fusion welding [5–8]. By contrast, Hastelloy X can be readily welded owing to its low Al and Ti contents.

However, the heat applied during the welding process may distort the properties of the alloy; this is prevented by repairing Hastelloy X through brazing. Owing to the low heating temperature, brazing does not induce strain-age cracking in components composed of Ni-based alloys. Therefore, brazing is the preferred method for repairing such components [9, 10].

Several types of brazing filler metals have been developed to manufacture components composed of Ni-based alloys. The primary chemical component of brazing filler metals is Ni-Cr-Fe, and B, Si, or P is the primary melting point depressant (MPD). Cu, Al, Ti, and rare earth elements are added to optimize the performance of brazed joints [11–16]. However, the strengths of brazed joints of Ni-based alloys with different brazing filler metals are different. For example, when 60% Inconel 738 as the matrix was combined with 40% DF4B (containing B as the MPD) and BNi-3 (containing B and Si as the MPD) as brazing filler metals, the strengths of the joints formed by wide-gap brazing were 832 MPa and 620 MPa, respectively [17]. The brazing of Ni-based alloys result in brazed joints through isothermal solidification, which is caused by the diffusion of MPDs in the brazing filler metal. The diffusion of

Recommended for publication by Commission XVII - Brazing, Soldering and Diffusion Bonding

✉ Zhiping Wang
   wangzhiping0626@163.com

1 School of Materials Science and Engineering, Shenyang University of Technology, Shenyang 110870, China

2 School of Aeronautical Engineering, Civil Aviation University of China, 2898 Jinbei Road, Dongli District, Tianjin 300300, China

MPDs is a key factor affecting the strength and properties of the joint. Moreover, the interaction between an MPD and a base metal at the interface varies with the chemical composition of the base metal, thereby influencing the mechanical properties of a brazed joint. For example, with BNi-2 (containing B and Si as MPD elements) as the brazing filler metal and Inconel 718 as the base metal, the tensile strength of the brazed joint obtained through transient liquid phase bonding is 482 MPa; with GH3039 as the base metal and BNi-2 as the brazing filler metal, the strength of the brazed joint is 785 MPa [17]. The interaction between the brazing filler metal and the base metal should be understood to develop maintenance technology for hot section components of aeroengines.

Hastelloy X is extensively used to manufacture hot section components of aeroengines [18, 19] through brazing. However, few studies have focused on the interaction between the brazing filler metal and the Hastelloy X base metal. Therefore, we investigated the influence of MPD elements chemical composition on the formation of brazed joints by using Hastelloy X as the base metal and three commonly used elements, namely, B, Si, and P—which can reduce melting—as MPDs.

2 Experimental procedure

In this study, we used three types of Ni brazing filler metal, namely, BNi-2, BNi-5, and BNi-7; the chemical compositions and melting points of the brazing filler metals are listed in Table 1. B, Si, and P were used as MPDs to produce the three types of brazing filler metal, respectively. Table 2 summarizes the chemical composition of plate-shaped and cylindrical Hastelloy X base metal samples. The cylindrical sample was used to perform the mechanical property test, and the plate-shaped sample was used for wetting/spreading trials. According to the composition and application temperature range of the brazing filler metal, the brazing temperature was fixed within 950 °C to 1250 °C for 15 min. All specimens were prepared in an atmosphere tube furnace (VTL 1700, Boyuntong Instrument Technology Co., Ltd, Nanjing, China). The furnace was evacuated to 1.5 Pa and backfilled with argon gas after the base metal and brazing filler metal were placed in the furnace. The base metal and brazing filler metal were then heated to the brazing temperature, held for 15 min, and finally cooled to room temperature.

The samples were embedded in epoxy and polished to a 0.5-μm finish through standard procedures, and the metallographies of the samples were then observed. Subsequently, the samples were etched in a solution of $CuCl_2$, HCl, and anhydrous ethanol to observe their microstructures. Confocal laser microscopy (OLS4100-3D, OLYMPUS, Japan) was used to observe the metallographies of the brazing joints. The chemical compositions of the brazing joints were analyzed through scanning electron microscopy (SEM; Sigma 300, Carl Zeiss, Germany) in combination with energy dispersive spectrometry (EDS). Tensile test was performed on brazing joints at room temperature using a mechanical test system (Instron 8802, Instron, USA), and the test method was in compliance with the ISO 6892-1 2019 standard. The test sample is illustrated in Fig. 1. Two cylindrical bars with diameter 10 mm were installed in a brazing fixture, which was filled with brazing filler metal in a gap with a width of 100 μm between two bars. The bars were held at 1150 °C, 1250 °C, and 1100 °C for 15 min to obtain a brazing joint. Thereafter, the bar was turned to the structure displayed in Fig. 1. The microstructure of the fracture in the test sample was observed through SEM.

Table 1 Chemical compositions and melting points of the three brazing filler metals

Brazing filler metal	Element (wt%)							Melting point (°C)
	Cr	B	Si	Fe	C	P	Ni Bal.	
BNi-2	7.0	3.1	4.5	3.0	0.06		82.34	999
BNi-5	19		10.2		0.06		70.74	1135
BNi-7	14				0.06	10	75.94	890

Table 2 Chemical composition of Hastelloy X

	Element							
	C	Si	Mn	P	S	Cu	Co	Cr
Weight (%)	0.084	0.045	0.43	0.006	0.009	0.012	1.03	21.20
	Element							
	Al	Ti	B	W	Fe	Mo	Ni	
Weight (%)	0.20	0.009	0.003	0.53	18.12	8.30	Bal.	
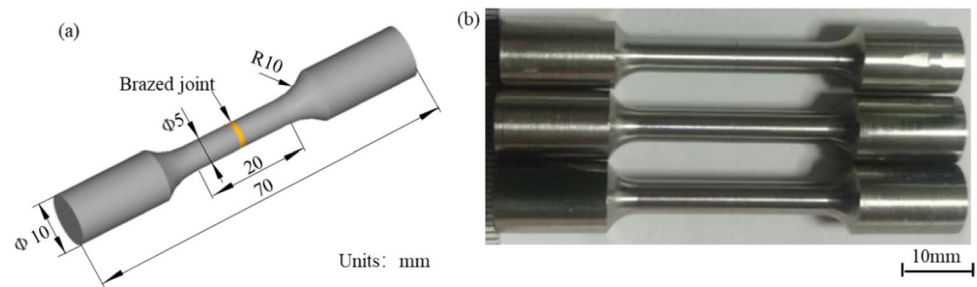
3 Results and discussion

3.1 Wettability analysis of the brazing filler metals

The wettability of the base metal is a key parameter that determines the effective spreading area of the brazing filler metal. Cracks in Ni alloy–based components are mostly manufactured through wide gap brazing, wherein the brazing filler metal and Ni-based powder is filled in the damaged area. The powder is in a nonmolten state in the high-temperature brazing process. After mixing, the powder diffuses with the brazing filler metal and affects its wettability [20–22]. Therefore, the appropriate brazing process should be determined to improve the properties of the joint formed through wide gap brazing and to ensure that the brazing filler metal has good wettability on the surface of the base metal.

Table 3 illustrates the wettability of the brazing filler metals on the surface of the Hastelloy X base metal; the symbol "–" in the table indicates that the brazing filler metal did not melt completely and the base metal was not wetted under the experimental conditions. The liquidus temperature of BNi-2 is approximately 1000 °C; however, the BNi-2 used in this study did not melt at 1000–1100 °C. Because oxidation occurs on the surface of the brazing filler metal, the melting point of the filler powder was increased. The wetting angle and thickness of the interaction layer were calculated by averaging the values of multiple samples through multiple measurements using metallographic imaging. As illustrated in Fig. 2, the thickness of the interaction layer was the maximum diffusion depth of the brazing filler metal below the original base metal surface.

Table 3 summarizes the wettability results, which were plotted as displayed in Fig. 3. According to Frenkel's liquid viscosity theory, the increase in temperature can cause a decrease in the binding energy between the atoms of the liquid structure and thus a decrease in the viscosity of the liquid; furthermore, the surface tension of the liquid decreased, and the fluidity of the liquid increased. According to the experimental results illustrated in Fig. 3a, the wetting angle exhibited a downward trend with the increase in temperature, indicating that the melting of the brazing filler metal intensified and spread with the increase in temperature, and the brazing filler metal interacted more strongly with the base metal. A wetting angle of 10° indicates good wetting between the brazing filler metal and the base metal, thereby enabling brazing. When the brazing temperature was increased from 950 to 1000 °C, the wetting angle of the BNi-7 brazing filler metal increased from 26.4 to 37.3°, and when the brazing temperature was increased to 1050 °C, the wetting angle sharply decreased to 2.7°. The change in wetting angle indicated that the melting degree of the BNi-7 brazing filler metal increased with the increase in temperature, and the liquid brazing filler metal exhibited maximum surface tension at 1000 °C. With further increase in temperature, the amount of melted brazing filler metal increased. The gravitational force of the liquid brazing filler metal was greater than the surface tension, thereby resulting in the complete spreading of the liquid brazing filler metal. Therefore, the wetting angle decreased sharply from 37.3 to 2.7°; when the brazing temperature reached 1100 °C, the measured wetting angle was 2.4°, which remained constant.

Table 3 Wettability test results

Brazing filler metal	Brazing temperature (°C)	Wetting angle (°)	Thickness of interaction layer (μm)
BNi-2	1000	–	–
	1050	–	–
	1100	–	–
	1150	8	148.99
	1200	11	151.50
BNi-5	1100	–	–
	1150	6.4	0
	1200	6	57.1
	1250	5.7	113.22
BNi-7	950	26.4	11.65
	1000	37.3	22.58
	1050	2.7	49.55
	1100	2.4	73.64

Fig. 2 Schematic of the wetting angle and thickness of the interaction layer
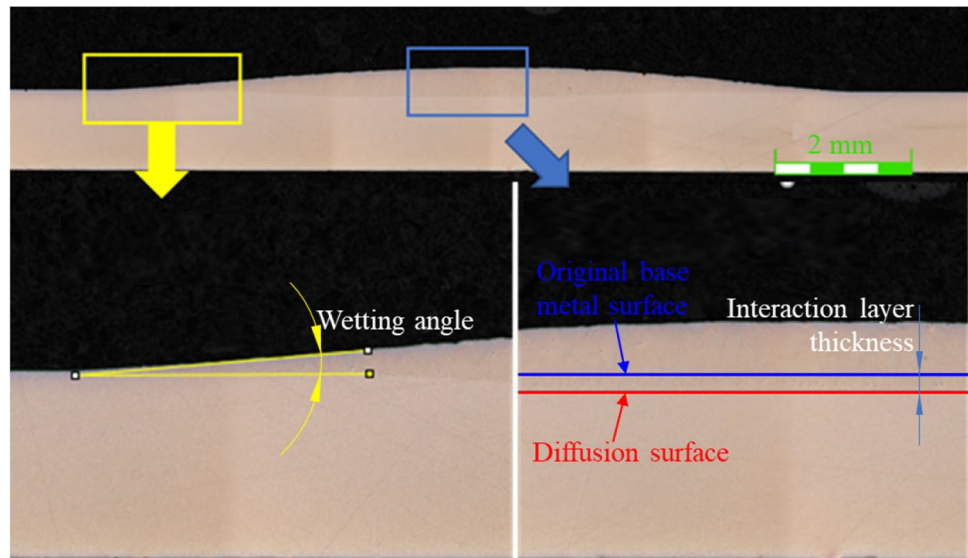
Fig. 3 Comparison of the **a** wetting angle and **b** interaction layer thickness among three types of brazing fillers at different temperatures
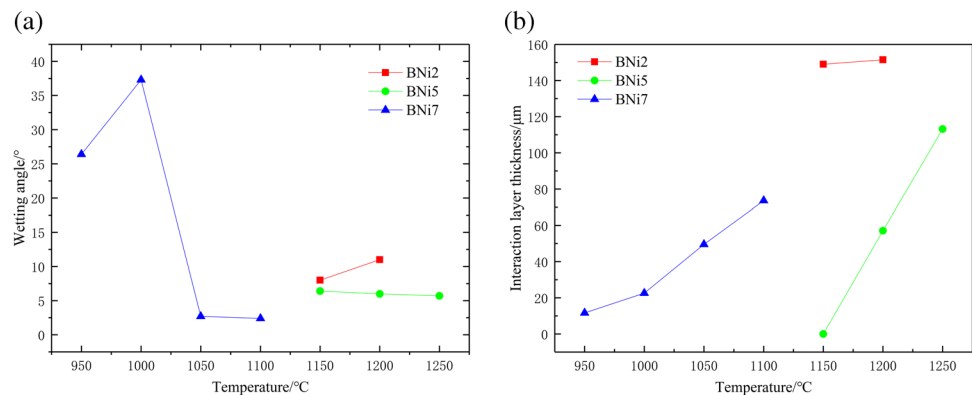
The BNi-7 liquid brazing filler metal completely wetted the base metal surface when the temperature exceeded 1050 °C. The minimum wetting angles of the BNi-2 and BNi-5 brazing fillers were approximately 8° and 6°, respectively, which were related to the heating temperature, composition of the brazing filler metal, and liquid structure.

Figure 3b displays the thicknesses of the interaction layers. The thickness of the interaction layer of the BNi-2 brazing filler metal was the largest (up to 150 μm). When the temperature increased from 1150 to 1200 °C, the thickness of the interaction layer slightly changed with temperature; the interaction layer was close to saturation under the experimental conditions. The thicknesses of the interaction layers formed by the BNi-5 and BNi-7 brazing filler metals increased notably with the increase in temperature and exhibited a nearly linear growth tendency, indicating that the interaction layer did not reach saturation under the experimental conditions. Moreover, the thickness of the interaction layer increased further with the extension of the holding time. The slopes of the three curves displayed in Fig. 3b

indicated that the saturation of the interaction between the BNi-2 brazing filler metal and base metal was considerably higher than that of the BNi-5 and BNi-7 brazing filler metals, indicating that the diffusivity of B is better than that of Si and P. Diffusivity is related to the size of diffusion atoms and diffusion potential energy. Therefore, the diffusivity of Si can be improved by increasing the temperature.

3.2 Metallographic analysis of the brazing filler metal wetting/spreading trials

Figure 4 illustrates the metallographic morphology of the BNi-2 brazing filler metal after spreading/wetting at 1150 °C. Figure 4 a, b, and c illustrate the global view, the end, and the middle section of the brazing filler metal, respectively, after wetting/spreading trials. The middle region of the spreading area was mainly composed of eutectic phase with dendritic morphology, whereas the eutectic phase at the end was mainly located in the top of the spreading area and had considerably lower concentration than that in the

Fig. 4 Cross-sectional image of BNi-2 after spreading/wetting at 1150 °C **a** global view, **b** end region, and **c** middle region
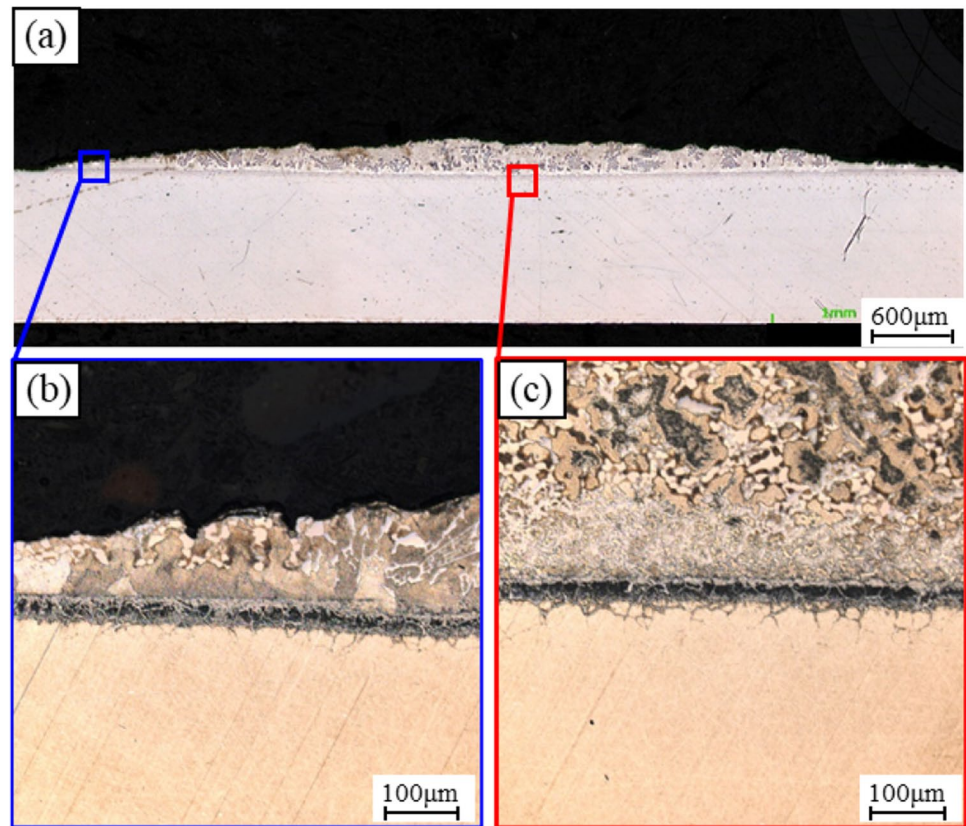

middle region. Solute enrichment was noted in the spreading area near the interface between the brazing filler metal and the base metal. However, the microstructure at the end of the brazing filler metal flow was not similar to that at the interface because the brazing filler metal in the middle region interacted with the base metal; B reduced melting in this region and diffused to the base metal and melted it to form a liquid film. The formation of the base metal liquid phase accelerated the diffusion of the brazing filler metal, thereby causing the diffusion of the brazing filler metal in other regions to the middle region. The diffusion distance and concentration of B in the solid base metal were considerably affected by the brazing holding time. The holding time of 15 min makes the diffusion of element B close to the saturated state, thereby resulting in the accumulation of solutes in the wetting/spreading area near the interface between the brazing filler metal and the base metal; this results in the formation of a solute-enriched area. During the brazing process, the brazing filler metal continuously melted and flowed to the ends and then interacted with the base metal after wetting and spreading. The diffusion time of the brazing filler metal at both end was insufficient, and thus, no obvious solute enrichment area was observed in both ends of the spreading/wetting area.

A black continuous B-rich diffusion zone was observed at the interface between the brazing filler metal and base metal, as illustrated in Figs. 4 and 5; the diffusion zone was observed in the joint formed by the BNi-2 brazing filler metal. In our pervious study, we observed the microstructure of a BNi-2 brazed joint at different high-temperature holding times, as displayed in Fig. 5; for a holding time of 0.5 h, a black diffusion zone was observed and gradually disappeared with an increase in the holding time. No black diffusion zone is observed for a long holding time because of the diffusion of an MPD into the base metal. Thus, the occurrence of a black diffusion zone is related to MPD content. Moreover, no black B rich diffusion zone was observed in the brazed joints with either the BNi-5 or BNi-7 brazing filler metal during spreading/wetting trials. Therefore, the formation of the black continuous region is related to B content in the brazing filler metal.

The black continuous band appeared in the interaction area between B in the brazing filler metal and the base metal; the region also constituted the main area of the diffusion layer. The diffusion layer was formed by the diffusion between the brazing filler metal and the base metal, but it did not include the region formed by the melting of the base metal and the isothermal solidification of the brazing filler metal. In the entire brazing process, the melting elements in the brazing filler metal continuously diffused into the base metal, thus melting the base metal surface and forming a liquid film. The liquid film was composed of a mixture of the
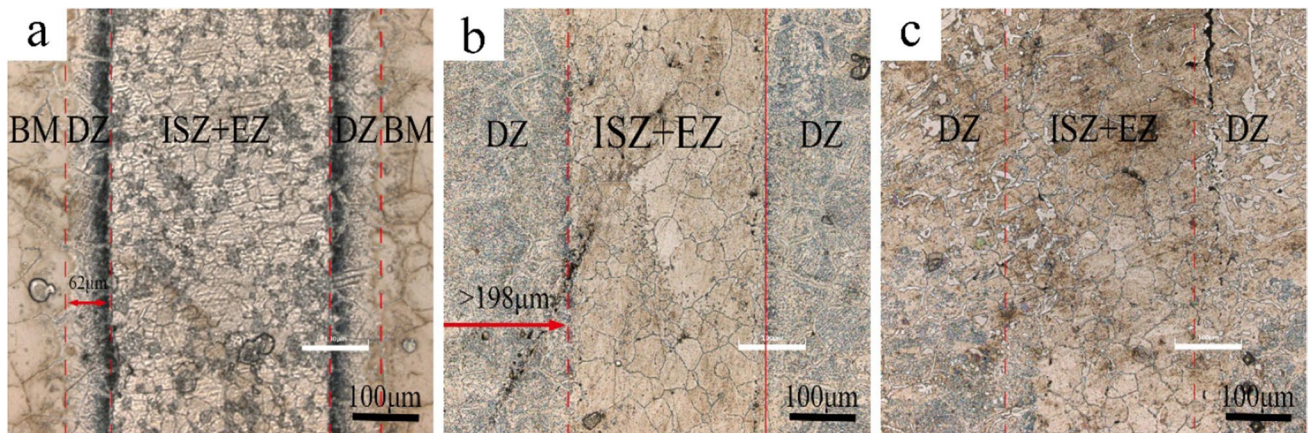
Fig. 5 Microstructure of the BNi-2 brazed joint at high-temperature holding times of **a** 0.5 h, **b** 2 h, and **c** 4 h

brazing filler metal and base metal components and provided a carrier for the subsequent diffusion of the elements in the brazing filler metal. With the extension of the holding time, the liquid film continued to move toward the base metal. The microstructure formed after the isothermal solidification of the liquid brazing filler metal because of the diffusion of elements that reduced melting. When the brazing was nearly complete and the liquid film no longer moved toward the base metal, the region centered on the liquid film formed the diffusion layer.

The black diffusion zone was "thin in the middle and thick at both ends," and the thickness of the diffusion layer at both ends ranged from 45 to 50 μm, and the thickness of the diffusion layer in the middle region was only 25–30 μm. Under the same test conditions, the diffusion capacity of B and the diffusion coefficient in the base metal remained constant. However, the thickness of the diffusion layer in the middle region was less than that at both ends, indicating that a large number of elements in the brazing filler metal were enriched at the middle of the interface. This promotes the diffusion of these elements into the base metal, thereby forming products with the constituent elements of the base metal and changing the phase structure of the diffusion layer, Thus, the thickness of the diffusion layer formed through the interaction between B in the middle and the base metal decreased, and the black continuous band diffusion layer was characterized as "thin in the middle and thick at both ends."

Figure 6 illustrates metallographic morphology of the BNi-2 brazing filler metal at 1200 °C. The morphology was identical to that at 1150 °C. Similarly, a black continuous band diffusion layer was observed between the brazing filler metal and the base metal

Figure 7 displays diffusion layer thicknesses at different brazing temperatures. The thickness of the diffusion layer in the middle ranged within 29–33 μm at a brazing temperature of 1150 °C; the thickness range was slightly lower than

that at a brazing temperature of 1200 °C. The increase in brazing temperature helped improve the maximum diffusion depth of B into the base metal at the middle of the brazing filler metal. The diffusion layer thickness at both ends ranged within 38–43 μm, which was slightly lower than the thickness at the brazing temperature of 1150 °C. Notably, the brazing temperature of 1200 °C accelerated the diffusion of elements because the elements in the brazing filler metal at the middle diffused into the base metal. Furthermore, the elements in the brazing filler metal at the end flowed toward the middle, the content of elements in the brazing filler metal decreased, and the diffusion layer thickness at the end of the trial at 1200 °C was lower than that at 1150 °C. In addition, when the molten brazing filler metal was in contact with the base metal, a liquid film was formed at the ends and the diffusion layer thickness increased in the middle of the diffusion layer was thicker. The middle of the diffusion layer gradually underwent isothermal solidification; the diffusion and interaction layers were "thin in the middle and thick at both ends."

Figure 8 illustrates the spreading/wetting metallographic morphology of the BNi-5 brazing filler metal at brazing temperatures of 1150 °C, 1200 °C, and 1250 °C. At 1150 °C, the brazing filler metal melted, infiltrated, and spread on the base metal, and obvious pores formed in the microstructure, as illustrated in Fig. 8a. The formation of pores indicated that the transformation of the BNi-5 brazing filler metal from the solid phase to the liquid phase at this temperature was not sufficient. The viscosity of molten brazing filler metal was high, and the fluidity was poor; thus, filling the small pores in the joint was difficult. With an increase in the brazing temperature, the degree of liquefaction of the brazing filler metal notably improved, the fluidity of the brazing filler metal increased, and the pore size in the brazed joint notably decreased at 1200 °C, as illustrated in Fig. 8b. When the temperature reached 1250 °C, few pores were observed

Fig. 6 Cross-sectional image of BNi-2 spreading/wetting at 1200 °C **a** global view, **b** end, and **c** middle region
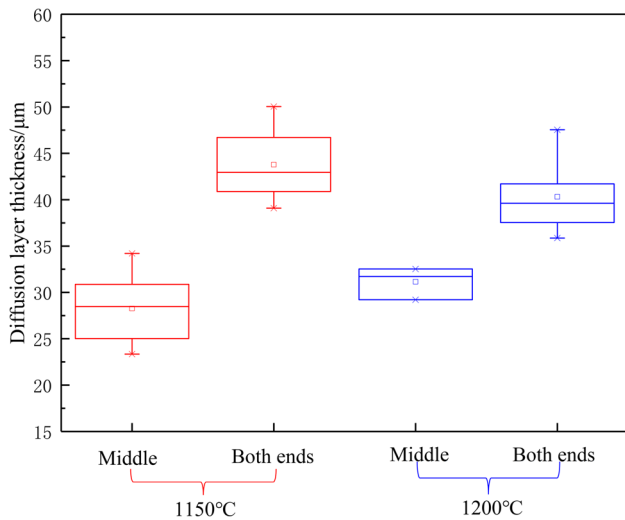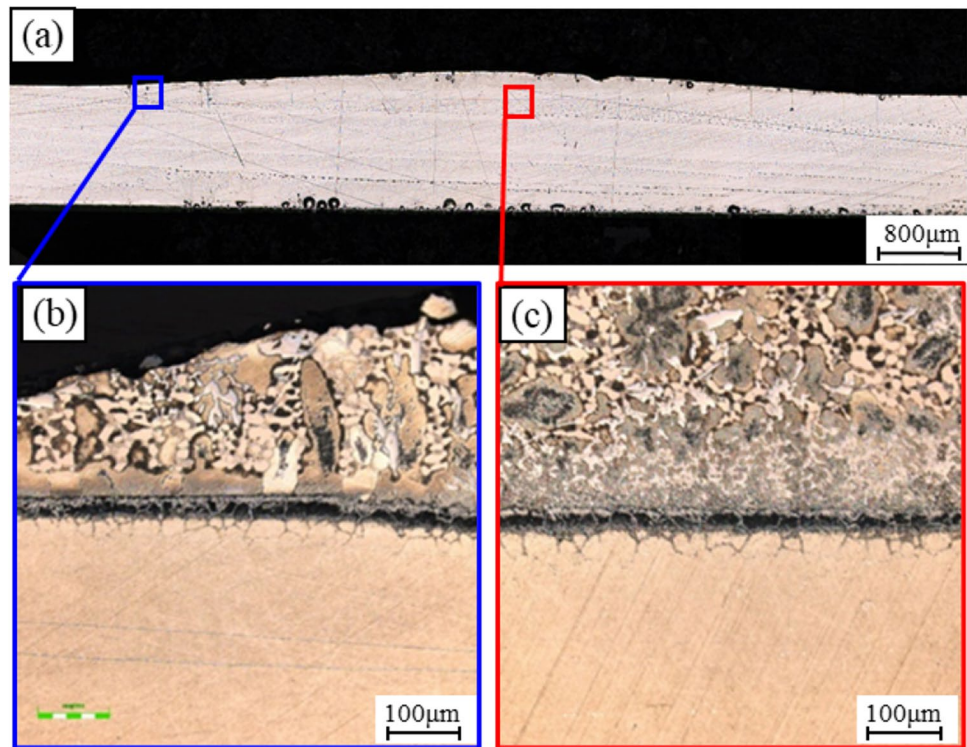
Fig. 7 Diffusion layer thicknesses of the BNi-2 brazing filler metal at different brazing temperatures

in the wetting/spreading trial, as depicted in Fig. 8c, indicating that the wettability and fluidity of the BNi-5 brazing filler metal at this temperature were sufficiently high to fill most of the pores, resulting in the reduction of brazing pore defects.

The BNi-5 brazing filler metal comprised Si as the MPD element, BNi-2 comprised B, and Si as MPD elements. The atomic size of Si is considerably larger than that of B, and

thus, the diffusivity of Si is lower than that of B. Therefore, the micrograph of the BNi-2 filler metal indicated the diffusion of B, and the micrograph of the BNi-5 filler metal indicated the diffusion of Si because BNi-5 comprised only Si as the MPD element. No obvious black continuous B-rich band similar to that in BNi-2 filler was observed in the BNi-5 filler mainly because of the change in the chemical composition of the diffusion layer. The interaction between BNi-5 and the base metal at the interface resulted in the formation of silicide, which was different from the interaction product of BNi-2. The diffusion layer thickness was considerably lower, and the diffusion layer thickness at 1150 °C was 8–9 μm, and the diffusion layer thickness at 1200 °C and 1250 °C was 10–11 μm. Although higher temperatures cause an increase in the diffusion layer thickness, the diffusion layer was close to saturation within 15 min of holding time when Si was used as the primary diffusion element. To further increase the diffusion layer thickness, the brazing holding time was extended. Moreover, at the same brazing temperature and holding time, the diffusivity of B was considerably higher than that of Si.

Figure 9 illustrates the metallographic morphology of the BNi-7 brazing filler metal after spreading/wetting at brazing temperatures of 950 °C, 1000 °C, 1050 °C, and 1100 °C. The microstructures of the brazing filler metal formed at 950 °C and 1000 °C were identical, and the microstructures of the brazing filler metal at 1050 °C and 1100 °C were identical. When the brazing temperature was lower than 1000 °C, the

Fig. 8 Cross-sectional images of BNi-5 after spreading/wetting at **a** 1150 °C, b 1200 °C, and **c** 1250 °C
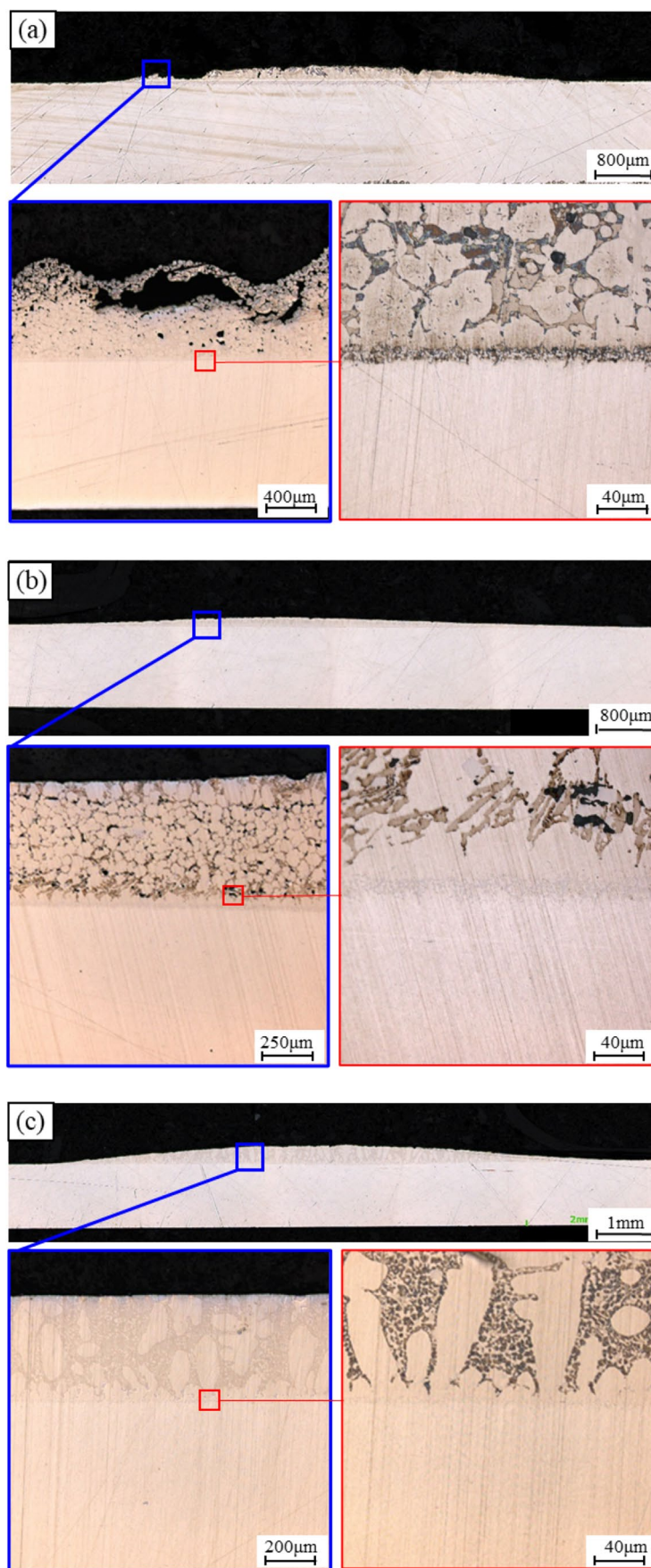
Fig. 9 Cross-sectional images of BNi-7 after spreading/wetting at **a** 950 °C, **b** 1000 °C, **c** 1050 °C, and **d** 1100 °C
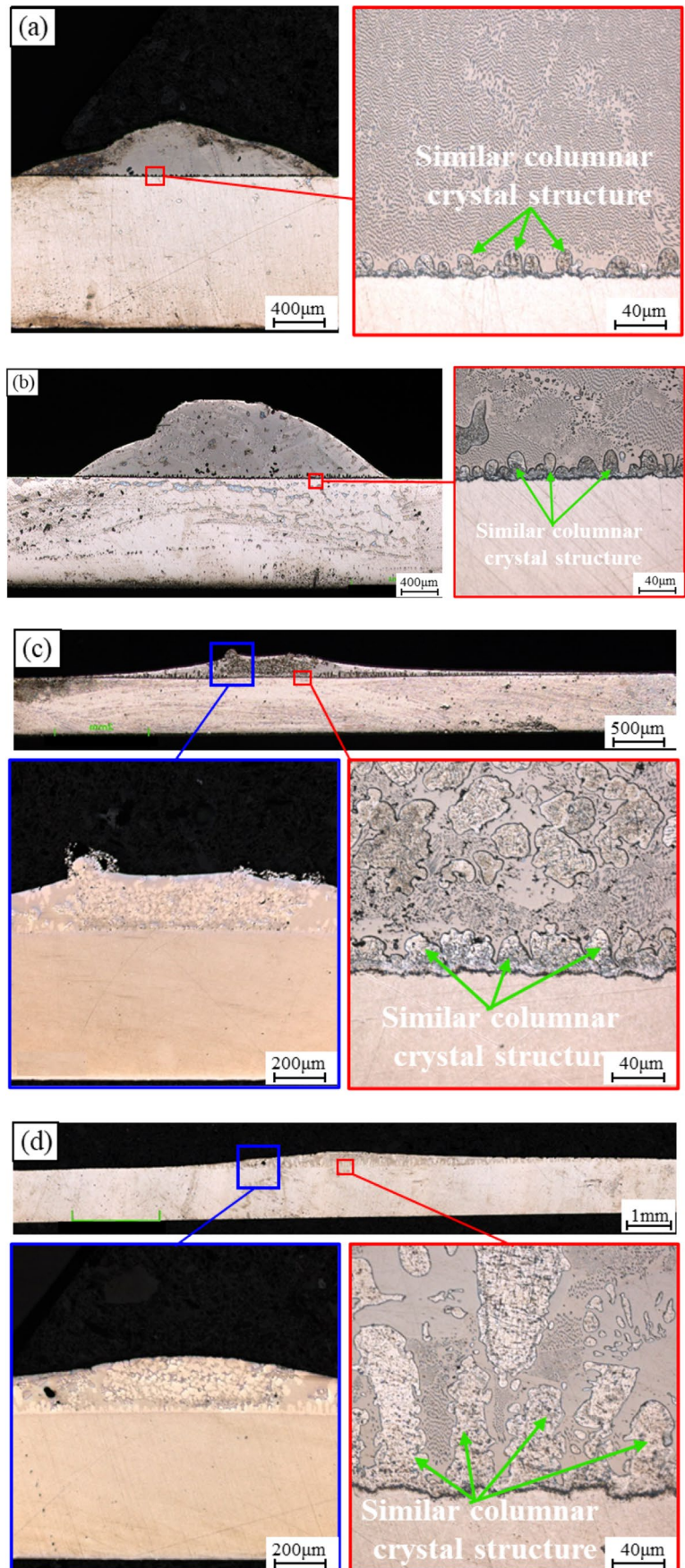
structure of the BNi-7 filler metal was uniform, dense, and free of pores; when the brazing temperature was higher than 1050 °C, a small number of pores appeared inside the brazing filler metal, and the microstructure was constituted by two phases—light and dark. The light phase was mainly concentrated in the middle region of the spreading area, and the darker phase was concentrated at the interface between the brazing filler metal and the base metal and the area where the brazing filler metal spread at both ends. Temperature had negligible effect on the morphology of the diffusion layer, and the interface between the brazing filler metal and the base metal exhibited a columnar crystalline structure. The size of the columnar crystal gradually increased with the increase in temperature. When the brazing temperature was higher than 1050 °C, the individual columnar crystals generated at the interface in the spreading region at both ends of the wetting area extended to the entire bonded area.

The BNi-7 brazing filler metal comprised P as the MPD element. Compared with the atomic radius of B (0.95 Å) and Si (1.34 Å), the atomic radius of P (1.30 Å) is similar to that of Si, but the melting point of P (590 °C) is considerably smaller than that of Si (1414 °C). Thus, BNi-7 required the lowest suitable brazing temperature among the three kinds of brazing filler metal. Therefore, at the brazing temperature of the BNi-7 brazing filler metal, P exhibited high diffusivity and completely diffused into the base metal.

3.3 Chemical composition of the brazing filler metal

The morphology of the BNi-2 filler was observed using SEM, as displayed in Fig. 10. The brazing microstructure

was uniform and represented a "gully" shape, which was mainly composed of a dark black phase labeled with "1" and a light gray phase labeled with "2," as displayed in Fig. 10a. A banded structure was observed at the interface, as illustrated in Fig. 10b. The EDS results are summarized in Table 4; the dark black phase labeled with "1" was a Ni-based solid solution, and the light gray phase labeled with "2" was primarily composed of Cr and B. The banded structure at the interface of the base metal and brazing filler metal, as displayed in Fig. 10b, was primarily composed of MPD elements B, Ni, and Cr, indicating an obvious interaction between the brazing filler metal and the base metal. In addition, the atomic fraction of B at the position labeled with "3," "4," and "5" exhibited a gradient decrease, indicating the diffusion of B from the brazing filler metal to the base metal, and it is concluded to be a compound of (Cr, Ni) B, i.e. a Cr-Ni boride phase, according to the atomic composition formed [23].

The morphology of the BNi-5 filler metal observed using the SEM is illustrated in Fig. 11. Figure 11 a and b display the SEM images of the upper middle region and the region near the joint interface, respectively. The EDS test results of the area marked in Fig. 11 are illustrated in Table 5. The contents of Si at position "1" and position "3" were relatively equal, and the contents of Si at position "2" and position "4" were similar. Because Si was transformed from the solid phase to the liquid phase during the solidification process, the content of Si increased in the post-solidification zone. We speculated that position "3" and position "4" were the first solidification zones, where Si migrated to position "3" after the solidification of position "4," resulting in an
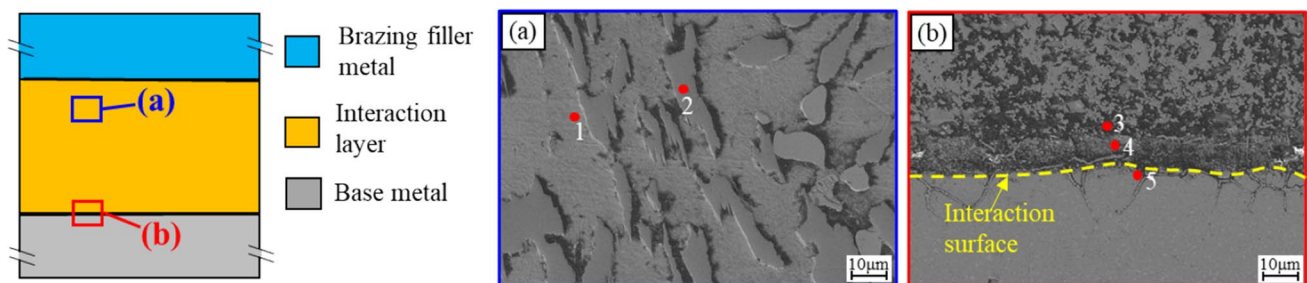
Fig. 10 SEM images of the morphology of the BNi-2 brazing filler metal **a** in the upper middle region and **b** near the interface of the joint

Table 4 Chemical composition of the BNi-2 filler metal

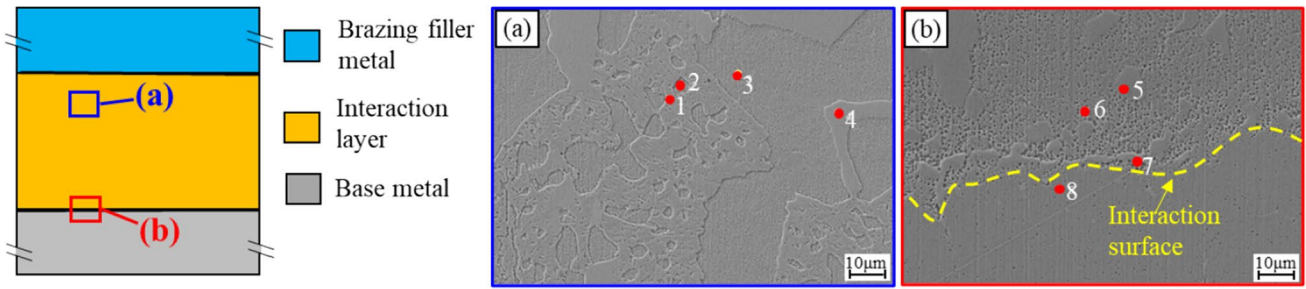| Position	Chemical composition at %					
	B	Si	Cr	Fe	Ni	Mo
1	-	3.03	14.65	-	82.32	-
2	48.02	2.01	27.85	8.35	13.77	-
3	63.87	1.87	15.82	2.15	16.29	-
4	41.83	-	20.02	7.67	23.04	7.44
5	29.91	-	32.44	1.31	29.35	6.99

Fig. 11 SEM images of the morphology of the BNi-5 brazing filler metal **a** in the upper middle region and **b** near the interface of the joint

Table 5 Chemical composition of the BNi-5 filler metal

Position	Chemical composition (%)				
	Si	Cr	Fe	Ni	Mo
1	21.35	24.76	5.71	48.18	-
2	12.99	25.59	3.28	58.14	-
3	20.01	21.20	3.42	55.37	-
4	13.37	40.99	3.98	37.42	4.24
5	21.19	26.49	-	48.72	3.6
6	12.94	26.57	4.67	55.82	-
7	8.52	28.69	3.86	47.71	11.22
8	-	25.33	21.17	50.17	3.33

increase in the Si content at position "3." The phases at position "1" and position "2" were formed during the cooling process after post-solidification. Because of the insufficient holding time, the microstructure in these areas was mostly characterized by liquid–solid mixing and nonisothermal solidification with a relatively high Si content in the liquid phase. The solid phase at position "2" solidified in the liquid–solid mixing zone, and the Si content in this area was relatively low, as illustrated in Table 5. The morphology at the joint interface is displayed in Fig. 11b; no obvious solute-enriched band structure was observed, indicating that the diffusion coefficient of Si is smaller than that of B. Moreover, the chemical composition at position "5" was identical to that at position "3," and a similar situation was

observed at position "6" and position "2." Si content at positions "5," "6," and "7" exhibited a gradient-like distribution, indicating the diffusion of Si from the brazing filler metal to the base metal. The presence of Si was hard to trace at positions farther away from the interface (e.g., position "8").

The morphology of the BNi-7 filler metal was observed using SEM, as illustrated in Fig. 12. The microstructure with a "water stain" was observed in the upper middle region after the spreading/wetting trial, as illustrated in Fig. 12a, indicating that the brazing filler metal possessed good spreading property. No obvious solute enrichment zone similar to that in the BNi-2 filler was observed near the joint interface, as displayed in Fig. 12b. According to the EDS results summarized in Table 6, the chemical compositions at position "1" and position "3" were identical, and the content of P was relatively high. The chemical compositions at position "2" and position "4" were similar, and the content of P was relatively low. This indicated that phases similar to those at positions "2" and "4" were first generated during the solidification process, and P diffused into the surrounding, resulting in the increase in P content in the phases similar to those at positions "1" and "3." Thereafter, the P-rich phases at positions "1" and "3" nucleated and grew during the cooling process. This isothermal solidification behavior induced by MPD element diffusion as observed in the microstructure of the three brazing filler metals, indicating that element diffusion was the dominant factor influencing the microstructure and properties of the brazed joint. At the positions near the
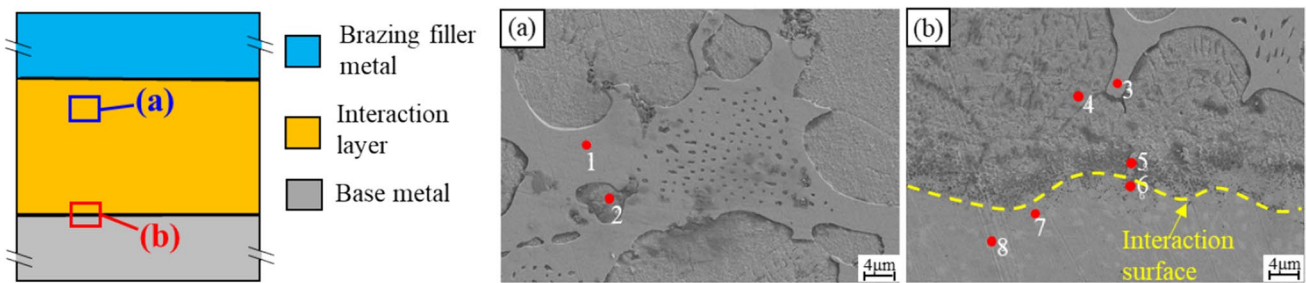

Fig. 12 SEM images of the morphology of the BNi-7 brazing filler metal **a** in the upper middle region and **b** near the interface of the joint

Table 6 Chemical composition of the BNi-7 filler metal

| Position	Chemical composition (%)					
	P	Cr	Fe	Ni	Mo	W
1	16.78	17.77	16.61	48.84	-	-
2	5.57	26.79	10.94	56.70	-	-
3	14.92	16.97	17.88	50.23	-	-
4	4.41	24.97	12.12	58.5	-	-
5	11.46	24.42	13.35	48.3	2.47	-
6	6.98	21.89	18.17	50.14	2.82	-
7	0.60	22.34	18.56	56.44	2.06	-
8	3.03	28.73	12.19	42.78	12.39	0.88

interface labeled as "5"–"7," the content of P exhibited a gradient decreasing distribution. Moreover, P was observed at the position far from the interface (e.g., at position "8"), indicating high diffusivity of P.

3.4 Diffusion behavior of the MPD elements B, Si, and P in Hastelloy X

According to the wettability test results, a higher temperature enables the spreading of the brazing filler metal to spread on the base metal surface, resulting in a lower wetting angle. The three MPD elements B, Si, and P promoted the melting of the base metal and formed a liquid film at the interface, thus providing a carrier for element diffusion. Furthermore, EDS results indicated that the Cr content in the three brazing filler metals was lower than that in the corresponding base metals; this enabled the diffusion of Cr from the base metal to the brazing filler metal. The atomic radius of Cr is 1.27 Å, which is similar to that of Si and P. The diffusion of Cr elements from the base metal into the brazing filler metal affects the coefficient of diffusion of the MPD elements into the base metal. Thus, the interaction layer was thin in the brazed zone formed by the BNi-5 and BNi-7 brazing filler metals. Therefore, with Hastelloy X as the base material, the brazing temperature should be lowered to reduce the diffusion of Cr elements from the base material to the brazed joint. Consequently, the diffusivity of the molten elements descending to the base material was affected, and the isothermal solidification time was shortened, thereby reducing the eutectic phase content in the joint and enhancing the mechanical properties of the joint.

3.5 Tensile strength of brazed joints

In the tensile test, all the samples were broken at the brazed joint. As illustrated in Fig. 13, no obvious yield period was observed in the load-displacement curves, indicating that brittle fracture occurred in the brazed joint. The tensile strengths of the brazed joints formed by BNi-2, BNi-5, and BNi-7 were 581.69 MPa, 498.45 MPa, and 496.09 MPa,
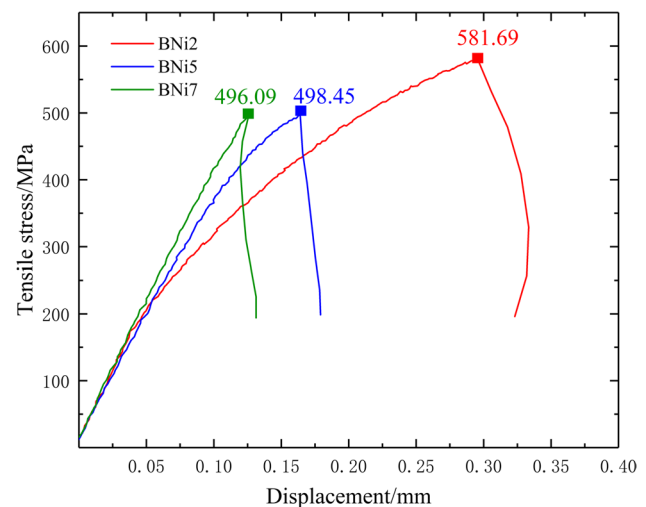
Fig. 13 Tensile characteristics of the brazed joints

respectively. The tensile strength of the brazed joint was consistent with the thickness of the interaction layer between the brazing filler metal and the base metal. Thus, the greater the interaction layer thickness, the higher the tensile strength of the brazed joint. A thicker interaction layer indicated a higher degree of interaction between the brazed joint and the base metal, which improved the tensile strength of the brazed joint.

As illustrated in Fig. 14, the fracture of the BNi-2 brazed joint was slightly uneven, and the fracture of the BNi-5 and BNi-7 brazed joint was relatively even and presented the characteristics of a large-area flat fracture. This was consistent with the tensile test results of the brazed joint. The strength of BNi-2 was the highest, and the strengths of BNi-5 and BNi-7 were similar. The fracture plane was relatively uniform with no dimples of ductile fracture, indicating the occurrence of brittle fracture.

Many sparse small pores were observed in the fracture initiation area of BNi-5 and BNi-7 brazed joints, as illustrated in Fig. 15. These were not observed in the fracture surface of the BNi-2 brazed joints. In addition, many

dendrites grew inside the pores. The EDS results of these dendrites are indicated by white boxes in Fig. 15 and illustrated in Table 7. The dendrites in the BNi-5 brazed joint consisted of silicon oxide, while the dendrites in BNi-7 were multicomponent mixtures, mainly consisting of chromium oxide. The pores were formed primarily because of the volume shrinkage during the liquid–solid transformation and the lack of liquid phase in the brazing filler metal. The remaining liquid phase was mostly a solute mixture with multiple components, which formed dendritic oxides during the cooling process. Furthermore, the BNi-5 brazed

joint was mainly composed of silicon oxide; the weak diffusivity of Si and its incomplete diffusion into the base metal resulted in a high Si content in the remaining liquid phase. By contrast, BNi-7 was primarily composed of chromium oxide with low P content, indicating that P completely diffused into the base metal, and Cr exhibited component segregation within the region. To avoid the aforementioned defects, the holding time of brazing can be appropriately extended; this can help homogenize the components of the brazed joint and thus improve its mechanical properties.
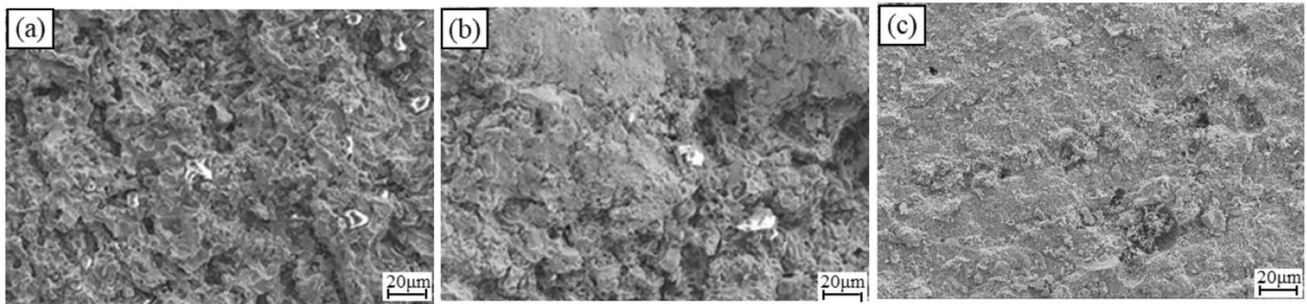

Fig. 14 Fracture morphology of the tensile test sample formed by **a** BNi-2, **b** BNi-5, and **c** BNi-7
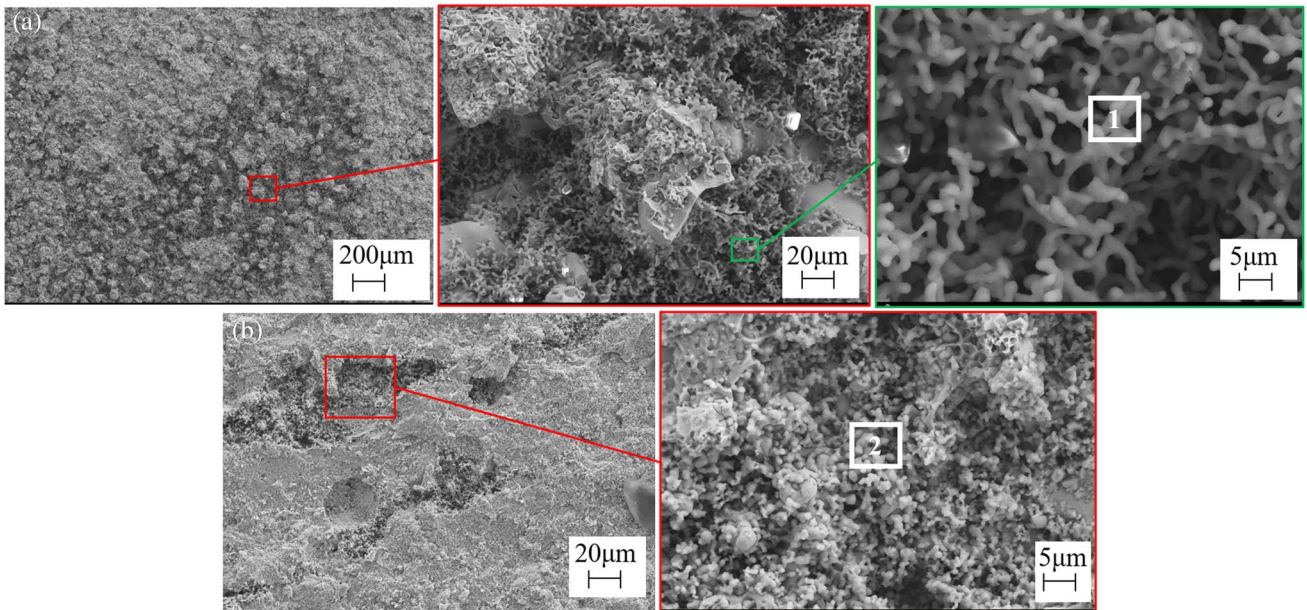

Fig. 15 Morphology of the fracture initiation area of the **a** BNi-5 and **b** BNi-7 brazed joints

Table 7 Chemical composition of the oxide formation illustrated in Fig. 15

Position	Chemical composition (%)								
	O	Si	P	Al	Ti	Cr	Mn	Fe	Ni
1	72.9	26.23	-	0.88	-	-	-	-	-
2	59.3	-	0.39	1.64	0.5	28.18	1	0.71	8.29

4 Conclusions

In this study, we used Hastelloy X as the base metal for brazing and analyzed the influence of three MPDs, namely, B, Si, and P, contained in Ni-based brazing filler metals on the formation of brazed joints. The main conclusions of the study are as follows:

(1) The wettability of each brazing filler metal containing B, Si, or P on the surface of Hastelloy X was different. The suitable brazing temperatures of BNi-2, BNi-5, and BNi-7 in an argon environment were 1150 ℃, 1250 ℃, and 1050 ℃, respectively. The corresponding tensile strengths of the brazed joints were 581.69 MPa, 498.45 MPa, and 496.09 MPa, respectively. This suggests that the brazing filler metal containing B as MPD achieves the best tensile strength.

(2) With a holding time of 15 min, the thickness of the interaction layer between the BNi-2 brazing filler metal and the base metal was approximately 150 μm, which was close to the saturation state. The interaction layer thicknesses of the BNi-5 and BNi-7 brazing filler metals increased further with an increase in the holding time, indicating that the diffusivity of B atoms is notably higher than that of Si and P atoms.

(3) The fracture of the brazed joints were brittle; this can be attributed to fine pore defects, most of which were dendritic oxides, at the fracture sources of BNi-5 and BNi-7.

Declarations

References

1. Bradley EF (1988) Superalloys: a technical guide. ASM International, United States
2. Donachie MJ, Donachie SJ (2002) Superalloys: a technical guide. ASM international
3. Gong L, Chen B, Du ZH, Zhang MS, Liu RC, Liu K (2018) Investigation of solidification and segregation characteristics of cast Ni-Base superalloy K417G. J Mater Sci Technol 34:541–550
4. Zhao LH, Tan Y, Shi S, Zhuang XP, Niu SQ, You QF, Wang YN (2019) High temperature oxidation behavior of electron beam smelted K417 superalloy. Vacuum 170:108979
5. Bi G, Sun C, Chen H, Ng F, Ma C (2014) Microstructure and tensile properties of superalloy IN100 fabricated by micro-laser aided additive manufacturing. Mater. Des. 60:401–408
6. Xie JL, Ma YC, Xing WW, Qu MQ, Zhang L, Liu K (2019) Microstructure and mechanical properties of a new cast nickel-based superalloy K4750 joint produced by gas tungsten arc welding process. J Mater Sci 54:3558–3571
7. Han K, Wang HQ, Shen L, Zhang BG (2018) Analysis of cracks in the electron beam welded joint of K465 nickel-base superalloy. Vacuum 157:21–30
8. Egbewande AT, Buckson RA, Ojo OA (2010) Analysis of laser beam weldability of Inconel 738 superalloy. Mater Charact 61:569–574
9. Song RK, Ma D, Wu SJ (2019) Microstructure, mechanical properties and thermal fatigue behavior of K417G alloy used in turbine guide vane. Rare Met Mater Eng 48:1517–1522 (in Chinese)
10. H Xiao, M Warren (2012) Wide gap braze repair of gas turbine blades and vanes-A review. Journalof engineering for gas turbines and power 134:010801.1–010801.17
11. Liu D, Song Y, Shi B, Zhang Q, Song X, Niu H, Feng J (2018) Vacuum brazing of Gh99 superalloy using graphene reinforced BNi-2 composite filler. J Mater Sci Technol 34:1843–1850
12. Wang FZ, Wang QZ, Yu BH, Xiao BL, Ma ZY (2011) Interface structure and mechanical properties of Ti(C, N)-based cermet and 17-4PH stainless steel joint brazed with nickel-base filler metal BNi-2. J Mater Process Technol 211:1804–1809
13. Yuan XJ, Kang CY, Kim MB (2009) Microstructure and XRD analysis of brazing joint for duplex stainless steel using a Ni-Si-B filler metal. Mater Charact 60:923–931
14. Li GJ, Zhang PL, Shi HC, Yu ZS (2018) Microstructure and properties of Cr18-Ni8 steel joints brazed with BN7 + 3% Cu composite solder. Vacuum. 148:303–311
15. Shi HC, Yu ZS, Cho JR (2018) A study on the microstructure and properties of brazing joint for Cr18-Ni8 steel using a BNi7 + 9% Cu mixed filler metal. Vacuum 151:226–232
16. Esmaeili H, Mirsalehi SE, Farzadi A (2018) Vacuum TLP bonding of Inconel 617 superalloy using Ni-Cr-Si-Fe-B filler metal: metallurgical structure and mechanical properties. Vacuum 152:305–311
17. Cheng Z, Li X, Wang B et al (2020) M3B2-type borides effect on the wide gap brazing of K417G alloy with mixed powder. J Alloys Compd 821:153431
18. Attalah MM, Jennings R, Wang X, Carter LN (2016) Additive manufacturing of Ni-based superalloys: the outstanding issues. MRS Bull 41:758–764
19. Herzog D, Seyda V, Wycisk E, Emmelmann C (2016) Additive manufacturing of metals. Acta Mater 117:371–392
20. Gasper AND, Hickman D, Ashcroft I, Sharma S, Wang X, Szost B, Johns D, Clare AT (2019) Oxide and spatter powder formation during laser powder bed fusion of Hastelloy X. Powder Technol 354:333–337
21. Gasper AND, Szost B, Wang X, Johns D, Sharma S, Clare AT, Ashcroft IA (2018) Spatter and oxide formation in laser powder bed fusion of Inconel 718. Addit Manuf 24:446–456
22. Zhang H, Gu D, Ma C, Xia M, Guo M (2019) Surface wettability and superhydrophobic characteristics of Ni-based nanocomposites fabricated by selective laser melting. Appl Surf Sci 476:151–160
23. Kim YH, Kim KT, Kim IH (2006) Effect of mixing ratio on mechanical properties of wide-gap brazed Ni-based superalloy with Ni-Si-B alloy powder. Key Eng Mater 306-308:935–940